



Conformational characteristics of cellulose sulfoacetate chains and their comparison with other cellulose derivatives

Alexander S. Gubarev · Olga V. Okatova ·
Galina F. Kolbina · Tatsiana A. Savitskaya ·
Dzmitry D. Hrynshpan · Georges M. Pavlov

Received: 13 July 2022 / Accepted: 12 December 2022 / Published online: 22 December 2022
© The Author(s), under exclusive licence to Springer Nature B.V. 2022

Abstract An amphiphilic cellulose derivative the sodium salt of cellulose sulfoacetate was studied in a wide range of molecular masses by the methods of molecular hydrodynamics. Molecular masses were determined from sedimentation-diffusion analysis. The cross and general scaling relationships were established in the studied range of molecular masses for intrinsic viscosity and coefficients of velocity sedimentation and translational diffusion, and molecular masses. The conformational characteristics of the chains, such as the persistence length, hydrodynamic diameter were established using the Multi-HYDFIT

suite applied to the entire set of experimental data. The features of using the Multi-HYDFIT suite for calculation of molecular mass per unit length of linear chains are discussed. The results obtained for this cellulose sulfoacetate series have been compared with literature data for other water-soluble cellulose derivatives using normalized scaling concept of intrinsic viscosity data. It has been shown that water-soluble cellulose derivatives form a community, which is characterized by virtually identical equilibrium sizes of rigid chains in aqueous solutions.

Supplementary Information The online version contains supplementary material available at <https://doi.org/10.1007/s10570-022-05000-y>.

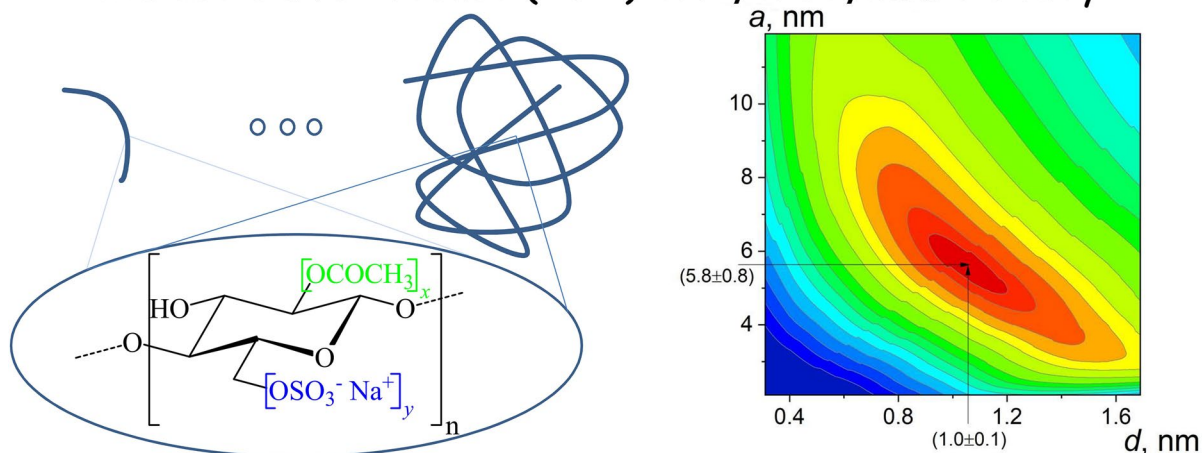
A. S. Gubarev
Department of Molecular Biophysics and Polymer Physics,
St. Petersburg State University, Universitetskaya Nab. 7/9,
St. Petersburg, Russia 199034

O. V. Okatova · G. F. Kolbina · G. M. Pavlov (✉)
Institute of Macromolecular Compounds, Russian
Academy of Sciences, Av. Bol'shoi 31, St. Petersburg,
Russia 199004
e-mail: georges.pavlov@mail.ru

T. A. Savitskaya · D. D. Hrynshpan
Research Institute of Physical and Chemical Problems,
Belarusian State University, Leningradskaya Str. 14,
220030 Minsk, Belarus

Graphical abstract

Cellulose SulfoAcetate (CSA) in Hydrodynamic Study



Keywords Water soluble cellulose derivatives · Molecular hydrodynamic methods · Multi-HYDFIT program application · Conformational characteristics

Introduction

Polysaccharides are a tremendous and diversified class of biopolymers that largely determine the type of existing life forms on Earth. They have long been a significant source of renewable chemical raw materials for use in a wide range of industries, both large-tonnage and high-tech. Polysaccharide macromolecules have different structure, covering all possible topologies and architectures of macromolecules and, accordingly, exhibiting a huge range of properties. Among the polysaccharides one can find very flexible and extremely rigid structures; linear and branched; uncharged and charged; homo- and hetero-molecules. The conformational states of polysaccharides are the result, firstly, of the particular features of their primary structure: (the type of pyranose ring bonding, variations in the arrangement of OH groups, the presence of different substituents of OH groups) and secondly, of the formation of multi-strand helical structures with maximum attainable chain rigidity. Thus, studying the polysaccharides is equivalent to diving into the general problems of polymer and biopolymer science. It is in the space of studying the individual properties of macromolecules that the interpenetration and mutual enrichment of polysaccharides science and polymer

science takes place. Among polysaccharides, cellulose occupies a special place, because it is the most spread organic polymer on Earth (Klemm et al. 2005).

Since ancient times, cellulose has been used in the form of various grades of paper and cotton fabrics, and in modern civilization such use of it is carried out in huge quantities. It is known that the use of cellulose has significantly expanded due to the synthesis and applications of a huge range of its derivatives.

Much attention of researchers is paid to the preparation and application of water-soluble cellulose derivatives. Various cellulose ethers (e.g., methylcellulose, hydroxypropylcellulose, carboxymethylcellulose) and esters (e.g., cellulose sulfate) are highly soluble in water and widely used commercially, for example, in the paint industry, as detergents, in cosmetics, foodstuffs and biomedical applications (Heinze and Liebert 2001; Heinze et al. 2003; Heinze 2005; Klemm et al. 2005; Arca et al. 2018; Rincón-Iglesias et al. 2019; Seddiqi et al. 2021).

A notable interest has been renewed in the synthesis and application of cellulose sulfoacetate and cellulose ether sulfates (Chauvelon et al. 2003; Thomas et al. 2003; Nascimento et al. 2012; Cao et al. 2016; Rohowsky et al. 2016). Since solutions of cellulose sulfoacetate, as well as solutions of other cellulose

derivatives, in some cases exhibit lyotropic and thermotropic mesomorphism, this may be associated with a significant equilibrium rigidity of their chains (Werbosj and Gray 1976; Gilbert and Patton 1983; Shimamoto et al. 2000; Grinshpan et al. 2005; Geng et al. 2013; Makarova et al. 2013; Ishii et al. 2019; Kádár et al. 2021). Determination of conformational characteristics, primarily the persistent length or the length of the statistical segment, requires a quantitative study of the homologous series of the corresponding linear polymer/polysaccharide by macromolecular physics methods.

This work concerns the study of promising derivative—the amphiphilic cellulose Na-sulfoacetate (CSA). CSA is able to form highly concentrated solutions in water (up to 60% *wt.*), in which a cholesteric mesophase is formed, as evidenced by the color of the solutions and by the results of rheological studies, which made it possible to establish an extreme dependence of viscosity on polymer concentration. The ordered supramolecular structures in the form of individual spherulites appear already in solutions with a concentration of 42%. With a further increase in concentration, they fit into spherulitic ribbons and more complex structural formations. As the concentration increases above 52%, the phases reverse, and the anisotropic phase becomes the continuous phase (Grinshpan et al. 2010).

So far as better part of lipids in biological membranes is in the liquid crystal (LC) phase, the ability of CSA to form ordered structures determines the possibility of using this polymer as a component of drug

systems, which has a structural similarity with the components of a cell and, therefore, is related to the human body (friendly polymer). Taking into account that CSA does not have acute toxicity (lethal dose 50 (LD 50) for mice and rats could not be determined), and besides, it does not have skin-irritating, skin-resorptive and allergenic effects, this cellulose derivative is seen as a good candidate for use as an excipient for the manufacture of hard and soft hydrophilic dosage forms. Thus, its use in this capacity made it possible for the first time to produce fast-dispersing dosage forms from medical activated carbons, which were approved for industrial production and medical use (Savitskaya et al. 2005, 2006). The results are demonstrated in Fig. 1.

In addition, CSA, being a polymeric cation exchanger, can enter into ion exchange reactions with cationic antibiotics of the penicillin, aminoglycoside, cephalosporin series, etc. In particular, it was shown that the complex of CSA with the aminoglycoside antibiotic kanamycin (CNM) demonstrates greater antibacterial activity compared to the standard form of CNM, which can be explained by the participation of only the monomeric form of the antibiotic in this complex (Savitskaya et al. 2021).

This work presents the results of studying samples and fractions of CSA synthesized by homogeneous synthesis, which were studied in the 60-fold range of molecular masses. Almost all the studied fractions belong to the region of transition of macromolecules from the mature coil to the model of a slightly bent

Fig. 1 Dispersion of activated carbon (AC) tablets in water. Left—AC tablet (0.22 g) modified by 0.018 g cellulose Na-sulfoacetate, right—a non-modified traditional tablet with starch as a binder



rod. This provides additional interpretative possibilities, which are demonstrated in the article.

The velocity sedimentation, translational diffusion, and viscous flow of dilute solutions of CSA in 0.2 M NaCl at 25 °C were studied. The set of experimental data was processed on the basis of the Multi-HYDFIT program developed by de la Torre (Ortega and de la Torre 2007; Amorós et al. 2011). As a result, estimates of the persistent length and hydrodynamic diameter of CSA chains were obtained. It is necessary to analyze the capabilities of the Multi-HYDFIT software to determine the shift factor (mass per unit length of glycoside chain) from a set of experimental data. Also for these purposes the set of CSA fractions in the range of low molecular masses was obtained and studied. The extension of the interval in this molecular mass region has revealed the features of the trend of the common dependence of water-soluble cellulose derivatives in normalized coordinates.

Finally, using the concept of normalized scaling relations for the most sensitive size characteristic—intrinsic viscosity, we compare the set of water-soluble cellulose derivatives, neutral or with suppressed polyelectrolyte effects, and show that they represent a commonality of linear chains of 1-4 glucans characterized by similar chain sizes in solutions.

Electronic Supplementary Information (ESI) file contains the processing of primary experimental data.

Experimental

Materials

Cellulose sulfoacetate-Na (CSA) samples were obtained by homogeneous synthesis of cellulose, obtained by the sulfate process. Bleached sulphate pulp made of coniferous wood ('Arkhangelsk Pulp and Paper Mill') extracted by the state standard (GOST 9571–89) with a viscose-average degree of polymerization 740 was used as the parent cellulose for derivatization (Grinshpan et al. 2010). 85% orthophosphoric acid, 96% sulfuric acid (SA), 98% acetic anhydride (AA) with the purity qualification p.a. were purchased from Sigma Aldrich (CAS Numbers 7664–38-2, 7664–93-9, 108–24-7, correspondingly). Solid sodium hydroxide (Sigma Aldridge, p.a., CAS number 1310–73-2) has been

utilized in the neutralization process. All chemicals were used as received.

The cellulose initially crushed and dried at 105 °C was loaded into a thermostatically controlled reactor and moistened with 85% orthophosphoric acid. The swollen cellulose mass was kept for 0.5 h at a temperature of 20 ± 2 °C, and then stirred for 2 h until a homogeneous 6% *wt.* solution was obtained. An esterifying mixture of 96% SA and AA was slowly added to the prepared solution with constant stirring. The volume ratio AA:SA was 10:1. The esterification temperature was maintained at 30–40 °C. After the introduction of the esterifying mixture, stirring was continued for 15 min. The mixture cooled to 20 ± 2 °C was poured into a large volume of aqueous sodium hydroxide solution with constant stirring and cooling until pH 7–7.5 was reached. The particles of non-esterified and therefore water-insoluble cellulose were removed by mechanical filtration. The filtrate was dialyzed and the polymer was isolated in solid form using a rotary evaporator under vacuum conditions at a temperature of 55 °C. The polymer yield was 95%. The samples were stored in a desiccator at a relative humidity of 2.5%.

CSA sample with $M_{SD} = 41000$ g/mol was fractionated by gradual fractional precipitation in the water-dioxane system. The reprecipitated fractions were freeze-dried to constant weight from aqueous solutions. As a result, 12 fractions readily soluble in water were obtained.

The content of acetate groups was determined from the proton magnetic resonance (PMR) spectra, and the proportion of sulfate groups was calculated from the sulfur content determined by elemental analysis (Grinshpan et al. 2010). The degrees of substitution were determined for 5 fractions, as a result, the following average estimates of the degrees of substitution were obtained: for acetate $x_{Acet} = 0.9 \pm 0.2$ and sulfate $y_{Sulf} = 1.2 \pm 0.1$ groups, which corresponds to the following structural formula of the repeating unit: $[C_6H_7O_2(OH)_{3-x-y}(OSO_3^-)_y(OCOCH_3)_x]Na^+$.

Fractionation proceeded by molecular mass (MM) and no systematic change in composition from MM was observed. At the same time, the spread of substitution degrees for acetate groups was greater than those for sulfate groups.

Methods

The CSA solutions exhibit clear viscous polyelectrolyte effects in pure water solution, the study of which will be presented in a separate work. To determine the reliable molecular and conformational characteristics of CSA, it is necessary to suppress polyelectrolyte effects; therefore, the corresponding researches were carried out in 0.2 M NaCl. The complex of hydrodynamic investigations including the study of translational friction (velocity sedimentation and translational diffusion) and rotational friction (viscous flow of dilute solution) was applied. The theoretical grounds of these methods and the approaches to the interpretation of experimental results are described in classical monographs (Tanford 1961; Tsvetkov et al. 1971; Cantor and Schimmel 1980) and in some our reviews (Pavlov et al. 2011; Pavlov 2016; Perevyazko et al. 2021).

Velocity sedimentation was investigated with MOM 3170 analytical ultracentrifuge (Hungary) in a double sector synthetic boundary cell (the height of the centerpiece was 12 mm) at a rotor speed of 40×10^3 rpm. The concentration dependence of the sedimentation coefficient s was studied for several fractions. It satisfied the linear approximation $s^{-1} = s_0^{-1}(1 + k_s c + \dots)$, where c is polymer concentration, and k_s is Gralen coefficient (see Figs. S1–S3 in ESI). The obtained Pavlov-Frenkel scaling relationship between s and the concentration sedimentation coefficient k_s was determined: $k_s = K_{sks} s_0^{(2-3b_s)/b_s} = 1.81 s_0^{3.4 \pm 0.5}$ (Pavlov and Frenkel 1982). This relation was used to allow for the concentration effect in measurements carried out at a single concentration. Besides, for this purpose serves the dimensionless parameter $k_s/[\eta]$ which average value was 1.5 ± 0.2 for the studied system (Fig. S4 in ESI).

The translational diffusion coefficient D was determined from the time dependencies of dispersion of the diffusion boundary formed in a glass cell with optical path length $l = 30$ mm at an average solution concentration $c = 0.04 \times 10^{-2}$ g/cm³. The D values obtained at these low concentrations were assumed to be the values at infinite dilution D_0 . Lebedev's polarizing interferometer (Tsvetkov et al. 1971) was used as an optical recording system of the solution-solvent boundary. The refractive index increment $\Delta n/\Delta c$ was determined from the area under the interference curve, and its average value was (0.10 ± 0.01) cm³/g at the wavelength $\lambda = 550$ nm.

Viscometric measurements were carried out in an Ostwald viscometer. The values of intrinsic viscosities $[\eta]$ are shown in Table 1. Huggins parameters k' show some increase with decreasing of $[\eta]$ values (see Fig. S5 in ESI). The density increment $(1 - \bar{v}\rho_0)$ (\bar{v} is partial specific volume of polymer, ρ_0 is solvent density) was determined in water and in 0.2 M NaCl solutions and resulted in virtually similar values: $(1 - \bar{v}\rho_0) = (0.47 \pm 0.02)$. The density of the solvent was $\rho_0 = 1.005$ g/cm³ and its viscosity was $\eta_0 = 0.909 \times 10^{-2}$ P.

Molecular masses were determined according to Svedberg equation:

$$M_{sD} = \frac{s_0}{D_0} \frac{RT}{(1 - \bar{v}\rho_0)}, \quad (1)$$

within 6% experimental error. The experimental data and molecular masses calculated with Eq. (1) are given in Table 1.

Results and discussion

Raw hydrodynamic data and their mutual congruence check

Determination of three/four hydrodynamic quantities ($[\eta]$, D_0 , s_0 and k_s) for a homologous series of samples/fractions in independent experiments makes it possible to exclude from consideration one of the key characteristic of the chains, namely their dimensions, by combining $[\eta]$, D_0 , s_0 in expression:

$$(R[D]^2[s][\eta])^{1/3} = R[s][\eta]^{1/3}/M^{2/3} = k_B \Phi_0^{1/3}/P_0 \equiv A_0, \quad (2)$$

where the characteristic values $[D]$ and $[s]$ are $[D] \equiv D_0 \eta_0/T$ and $[s] \equiv s_0 \eta_0/(1 - \bar{v}\rho_0)$, R is the gas constant, k_B is the Boltzmann constant, Φ_0 and P_0 are Flory parameters. The A_0 value does not contain and does not depend on chain dimensions under the assumption of their equivalence in the compared experiments. This combination is the so-called hydrodynamic invariant A_0 . The A_0 values fluctuate in the polymer homologous series, but somewhat changes in the series of flexible-chain, rigid-chain, and globular polymer systems. Similarly, the union of D_0 , s_0 and k_s in the form of the relation $N_A(R^{-2}[D]^2[s]k_s)^{1/3} = N_A[s](k_s/M^2)^{1/3} = B^{1/3}/P_0 \equiv \beta_s$ is a

Table 1 Hydrodynamic characteristics ($[\eta]$, D_0 , s_0 , k_s), molecular masses (M_{sD}), hydrodynamic invariants (A_0 , β_s), and number of statistical segments in the chains (L/A) of CSA fractions and samples in 0.2 M NaCl at 25 °C*

N	$[\eta]$, cm ³ /g	$s_0 10^{13}$, s	k_s , cm ³ /g	$D_0 10^7$, cm ² /s	$M_{sD} 10^{-3}$, g/mol	$A_0 10^{10}$	$\beta_s 10^{-7}$	L/A^{***}
1	78	3.6	110	2.5	76	2.97	1.12	10.4
2	64	3.4		3.2	56	3.21		7.7
3**	67	3.0		3.55	45	3.36		6.1
4	60	3.0		3.7	43	3.33		5.9
5	59	3.2	98	4.0	42	3.56	1.42	5.8
6**	44	3.0		3.9	41	3.11		5.7
7	51	2.8		4.0	37	3.24		5.1
8	42	2.8	56	4.2	35	3.14	1.16	4.9
9**	35	3.2		5.6	30	3.74		4.2
10	44	2.7		5.2	27	3.63		3.7
11	36	2.7	69	5.2	27	3.40	1.42	3.7
12	23	2.2		7.4	16	3.46		2.2
13	14	2.0	16	7.6	14	2.89	1.02	2
14	10	1.6		15.0	5.6	3.77		0.8
15	-	1.1		46.5	1.25			0.2

*The experimental error of the initial hydrodynamic characteristics ($[\eta]$, s_0 and D_0) is under 3%, the Gralen coefficient k_s and molecular mass M_{sD} are determined within 10 and 6%, correspondingly; **non fractionated samples, all other fractions were obtained by fractionating sample 6; *** the statistical segment length A is twice of the persistence length a : $A = 2a$

sedimentation parameter that has the same properties as A_0 . Here B is Burgers parameter (Perevyazko et al. 2021). Some fluctuation of the parameters A_0 and β_s in the series of polymer homologues indicates the mutual compatibility of the obtained hydrodynamic characteristics ($[\eta]$, D_0 , s_0 and k_s). For the studied CSA series, the following average values of hydrodynamic invariants were obtained: $A_0 = (3.34 \pm 0.07)10^{-10}$ and $\beta_s = (1.23 \pm 0.08)10^7$, which are in good agreement with the literature data (Tsvetkov et al. 1984; Tsvetkov 1989; Pavlov and Frenkel 1995; Pavlov 1997; Grube et al. 2020). The hydrodynamic invariants calculated with Eq. (2) are given in Table 1. The error of their determination was under 10%.

After making sure that the hydrodynamic characteristics are consistent, one can proceed to further interpretation of the obtained matrix of experimental hydrodynamic values and molecular masses of polymer homologues.

Hydrodynamic scaling relationships

The comparison of hydrodynamic characteristics of macromolecules with each other and with molecular mass allows to obtain two types of scaling

Table 2 Parameters of scaling relationships for CSA molecules in 0.2 M NaCl solutions

$P_j - P_i$	$\lg K_i$	b_i	r_i^*
$[\eta] - s_0$	$-(0.11 \pm 0.06)$	0.35 ± 0.04	0.942
$[\eta] - D_0$	1.82 ± 0.01	$-(0.72 \pm 0.06)$	-0.959
$D_0 - s_0$	0.73 ± 0.02	$-(0.42 \pm 0.03)$	-0.970
$k_s - s_0$	0.26 ± 0.2	3.4 ± 0.5	0.966
$M - [\eta]$	$-(2.3 \pm 0.3)$	0.88 ± 0.07	0.966
$M - D_0$	3.71 ± 0.1	$-(0.68 \pm 0.02)$	-0.994
$M - s_0$	$-(1.0 \pm 0.1)$	0.32 ± 0.02	0.969

* r_i are the linear correlation coefficients of corresponding double logarithmic dependences

relationships. One is well known relationships between hydrodynamic characteristics and molecular masses or Kuhn-Mark-Houwink-Sakurada (KMHS) relations. Other type is cross relationships among hydrodynamic characteristics. Altogether, they may be given as follows: $P_i = K_{ij} P_j^{b_{ij}}$, where P_i is one of the hydrodynamic characteristics $[\eta]$, D_0 , s_0 , k_s and P_j is another corresponding hydrodynamic characteristic or corresponding molecular mass. Cross plots make it possible to verify how much the pair of initial characteristics obtained by various hydrodynamic methods

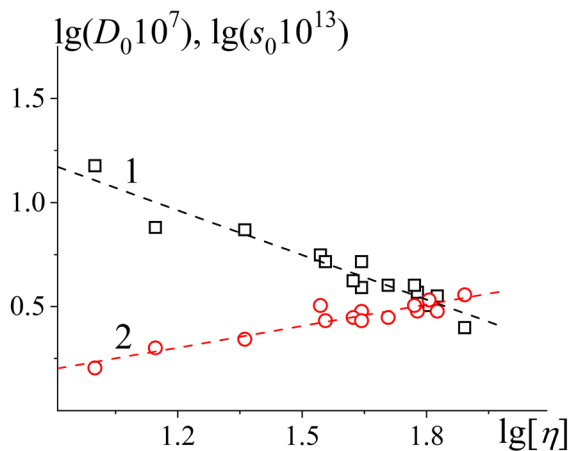


Fig. 2 Cross-scaling plots between the pairs of experimental values for the CSA molecules in 0.2 M NaCl solutions: $D_0=f_1$ ($[\eta]$) (1) and $s_0=f_2$ ($[\eta]$) (2)

correlate with each other. The case of a noticeable deviation of some pair of them indicates the need to verify the experimental specific results. An example of such cross-correlations is shown in Fig. 2. Table 2 summarizes the parameters of the entire set of derived scaling relationships for CSA molecules in 0.2 M NaCl solutions, which demonstrate fairly good cross-correlations between various experimental characteristics.

Based on the results of fractionation and the M_{sD} values, determined for each fraction, the molecular masses of three averages M_n , M_w and M_z were calculated and the sample inhomogeneity parameters $M_w/M_n = 1.83$ and $M_z/M_w = 1.18$ were calculated. These quantities characterize the low polydispersity of the initial sample. It can be expected that the polydispersity of fractions will be noticeably less. In this case, the deviation of M_{sD} from M_w for CSA fractions will be no more than 20% ($M_w/M_{sD} \lesssim 1.2$), for a number of CSA fractions, which is characterized by the index $b_\eta \approx 0.9$ (Sutter and Kuppel 1971; Skazka 1985).

Thus, the following canonical KMHS relations were obtained (see Fig. S6 in ESI):

$$\begin{aligned} [\eta] &= 4.48 \times 10^{-3} M^{0.88 \pm 0.07} \\ D_0 &= 5.11 \times 10^{-4} M^{-(0.68 \pm 0.02)} \\ s_0 &= 9.66 \times 10^{-15} M^{0.32 \pm 0.02} \end{aligned} \quad (3)$$

Further interpretation is to establish the conformational characteristics of the CSA chains, namely, the length of the statistical segment ($A = 2a$) or persistent length (a), and the hydrodynamic diameter (d).

Deviations of b_η from 0.50 (Eq. 3) for cellulose derivatives were discussed in detail and sharply in the late 60 s of the twentieth century. In principle deviations of b_η towards larger values, than 0.5 can be associated both with increased equilibrium rigidity of the chains, and/or with bulk interactions within one chain (intrachain excluded volume effects). Depending on the adoption of one or another point of view, we arrive at different estimates of the equilibrium stiffness of chains from the same data set. This discussion concerning cellulose derivatives is most fully described in (Flory 1966; Tsvetkov 1969). The conclusion of this discussion is the recognition that the reason for the deviation of b_η from 0.50 is mainly the effects of intrachain draining of cellulose chains or in general β 1–4 glucans, i.e. the high equilibrium rigidity of such chains, rather than the manifestation of bulk interaction effects in them. Note that Staudinger, introducing the concept of intrinsic viscosity as $\lim_{c \rightarrow 0} (\eta_{sp}/c) \equiv [\eta] = KM$, believed that this value is directly proportional to the mass of the macromolecule, which produce the friction in solution, i.e. in modern notation $b_\eta = 1$. It was the play of lucky chance that Staudinger came to this conclusion while studying cellulose nitrates, for which it was subsequently experimentally confirmed, that $b_\eta \approx 1$ for highly substituted cellulose nitrates. Note that highly substituted cellulose nitrates exhibit the highest equilibrium chain rigidity among all cellulose derivatives.

In this work, we will determine the equilibrium rigidity of CSA chains using the Multi-HYDFIT suite based on Monte Carlo Simulations using a worm-like model when processing the entire array of hydrodynamic data (Ortega and de la Torre 2007; Amorós et al. 2011). In this method, a common solution is sought that best fits the experimental data obtained by several independent methods, in our case, data on the translational friction of macromolecules in solutions (velocity sedimentation and translational diffusion), as well as the results of their viscous friction in dilute solutions (intrinsic viscosity).

Determination of conformational characteristics of CSA macromolecules with multi-HYDFIT suite

Hydrodynamic coefficients, solution properties and ultimately conformational parameters of the macromolecules can be predicted using Multi-HYDFIT – the universal model-analytical tool that employs Monte Carlo simulation, coupled to bead-model hydrodynamic calculations (Ortega and de la Torre 2007; Amorós et al. 2011). The program Multi-HYDFIT allows processing hydrodynamic data for practically any sort of macromolecules, covering the full range of the worm-like model, from short cylinders to very long, fully flexible chains. The main block of hydrodynamic data ($[\eta]$, D_0 , s_0 and M_{SD}) is entered into the program, as well as the system parameters η_0 , ρ_0 , \bar{v} and T , necessary to pass to the characteristic values $[D]$ and $[s]$.

The persistence length (a), transversal diameter (d) of a chain and mass per unit length (M_L) can be evaluated using Multi-HYDFIT program; this program performs a minimization procedure aimed at finding the best values of a , d and M_L satisfying the conditions of the chosen theoretical model. The Multi-HYDFIT program then “floats” the variable parameters in order to find a minimum of the multi-sample target function Δ^2 , which is calculated using equivalent radii:

$$\Delta^2(a, M_L, d) = \frac{1}{N_s} \sum_{i=1}^{N_s} \left[\left(\sum_Y w_Y \right)^{-1} \sum_Y w_Y \left(\frac{a_{Y(\text{cal})} - a_{Y(\text{exp})}}{a_{Y(\text{exp})}} \right)^2 \right], \quad (4)$$

where a_Y is the equivalent radius (defined as a radius of an equivalent sphere having the same value as the determined characteristic Y (translation diffusion D_0 , velocity sedimentation coefficients s_0 and intrinsic viscosity $[\eta]$)), N_s is the overall number of samples, w_Y is the weights for the various hydrodynamic properties, the indexes ‘cal’ and ‘exp’ indicate calculated and experimental values, correspondingly. The error function Δ is a dimensionless estimate of the agreement between the experimentally measured characteristic and the theoretical values of a , d and M_L calculated for the selected hydrodynamic characteristic and for a particular molar mass. Thus, 100Δ can be regarded as a typical difference between the calculated and experimental values for the whole set of properties of the series of samples. Multi-HYDFIT allows to fit any of the parameters (a , d and M_L) or fix

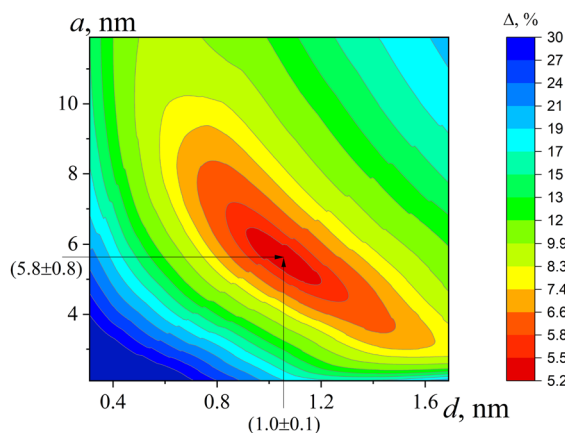


Fig. 3 The contour plot in dependence of Δ function values (error function Δ is represented as color gradient), obtained by Monte Carlo calculations for wormlike chains with excluded-volume effects. The plot was obtained with Multi-HYDFIT latest version (v. 3.0)

the value of either one of them to calculate the other two.

The final results of Multi-HYDFIT program are presented as the color gradient maps of conformation-structural parameters like a topographic map (Fig. 3). The color gradient is set by the value of the error function, consequently the solution is presented by the region with the lowest value of Δ . This is illustrated in Fig. 3 which demonstrates the result of Multi-HYDFIT handling hydrodynamic data obtained for CSA samples in dilute solutions. The measurements were performed using methods of molecular hydrodynamics (viscometry, isothermal diffusion and velocity sedimentation) with well-defined samples in the following molar mass range: $1\,250 < M, \text{ g mol}^{-1} < 76\,000$.

It shows the results of the program implementation to the CSA homologous series for resolving their main structural parameters considering a wormlike chain model: a – the persistence length and d – its transversal diameter. For the average composition of CSA, the mass of the repeating unit $M_0 = 322 \text{ g mol}^{-1}$ and the mass per unit length of the polymer chain (or linear density) of CSA $M_L = 6.2 \times 10^9 \text{ g mol}^{-1} \text{ cm}^{-1} = 620 \text{ g mol}^{-1} \text{ nm}^{-1}$ was calculated as the ratio of M_0 to the projection of monomer unit on the direction of fully extended β 1–4 glucan chain. Table 3 presents the results obtained with MULTY-Hydfit program in regard to the persistence length values were found

Table 3 The structural parameters of CSA chains determined with Multi-HYDFIT program: persistence length (a), transversal diameter of a chain (d), mass per unit length of chain (M_L) and target delta function (Δ)

n	Fractions in calculations	Variables	Fixed values	a , nm	d , nm	M_L , g mol ⁻¹ nm ⁻¹	Δ , %
1	1–15	a, d, M_L	–	6.7 ± 1.0	0.7 ± 0.5	600 ± 80	6.4
2	1–15	a, d	M_L	6.8 ± 1.3	0.8 ± 0.2	620	6.6
3	1–14	a, d, M_L	–	$*3.8 \pm 1.0$	0.7 ± 2.0	$*490 \pm 60$	5.2
4	1–14	a, d	M_L	5.8 ± 0.8	1.0 ± 0.1	620	5.4

*in our opinion, these estimations are rather not appropriate to the β 1–4 glucans structure

consistent in both calculation without and with a fixed parameter.

The principal set of hydrodynamic data was obtained for 14 samples and fractions, the 15th fraction was characterized only by translational friction methods due to its extremely minimal amount. However, the 15th fraction increases the molecular masses interval by a factor of 4.5 and its role in the statistical processing of the results becomes very high. Therefore, the obtained data were processed both with and without taking into account this 15th fraction. The processing results are presented in Table 3. Processing was carried out in two ways, firstly, by floating all variables (a , d and M_L), and secondly, with fixing the M_L value calculated from chemical structure of repeat unit. The treatment of all 15 fractions data (lines 1 and 2 in Table 3) allows us to set of results which are in good agreement with each other. Particularly noteworthy is the virtual agreement between the M_L value estimated by Multi-HYDFIT program and the M_L obtained from the structural formula of the CSA repeating unit. When processing the data without the last 15th fraction (1–14 fractions, Table 1) and without fixing the variables (a , d and M_L), we arrive at a noticeably smaller of the M_L value and, accordingly, a smaller persistent length of the chain. Note that in hydrodynamic theories, the quantities M_L and a are determined not independently, but as the ratio M_L/a , so the shifted estimate of M_L leads to a shifted estimate of the persistence length. At the same time, the processing of the same data array (1–14) with a fixed structural value of M_L leads to a persistent length estimate consistent within the error with the values given in lines 1 and 2 of Table. 3. This comparison leads to an important conclusion that a reliable estimate of M_L can be obtained from hydrodynamic data if there is a sufficiently wide set of data in the $L/A < 2$ region.

Such an estimate is also very sensitive to the statistics of the data in this area.

Thus, the combined processing of data on translational and rotational friction of CSA chains leads to the following estimate of the length of the statistical segment $A = 2a = (12 \pm 2)$ nm. The last column of Table 1 gives the number of statistical segments in the chain of the fractions, which shows that all the studied fractions/samples belong to the region of short and very short chains. It is the presence of several fractions for which $L/A < 2$, that leads, in our opinion, to a reasonable estimate of the mass per unit length M_L , which practically agrees with the calculated value.

Comparison of size of different water-soluble cellulose derivatives

Water-soluble cellulose derivatives represent a fairly large group of cellulose derivatives, which have long been used in a variety of ways. In our opinion, it is advisable to consider them together and identify their common properties/characteristics. For this purpose, we used the concept of normalized scaling relations as applied to intrinsic viscosity as the most sensitive characteristic to the dimensions of linear chains. The Yamakawa shift factor or the linear density of the polymer chain (M_L) was taken as a normalization parameter.

Let us compare the hydrodynamic characteristics of CSA with the data of some other water-soluble cellulose derivatives (Uda and Meyerhoff 1961; Brown and Henley 1964; Pavlov et al. 1995, 2004). The comparison will be made on the basis of intrinsic viscosity values, which are most sensitive to the size of the chains. We will use the concept of normalized scaling relations, which allows to obtain a size scan of all

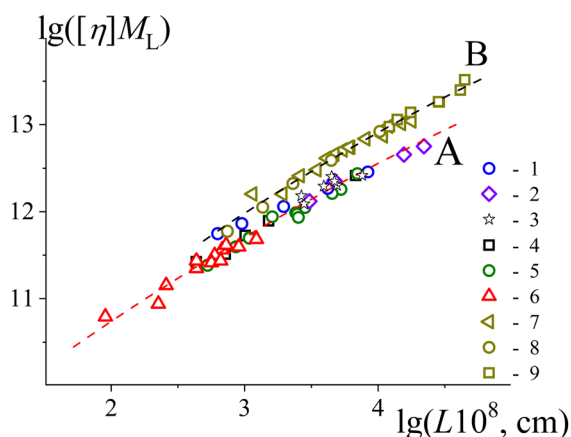


Fig. 4 Normalized KMHS relationship for linear density M_L of the cellulose derivatives chains: A – water soluble derivatives: 1 – methyl cellulose in H_2O (Uda and Meyerhoff 1961), 2 – sodium carboxymethyl cellulose in aqueous sodium chloride solutions (Brown and Henley 1964), 3 – sodium carboxymethyl cellulose with different degrees of substitutions in aqueous sodium chloride solutions (Barba et al. 2002), 4 – hydroxypropylmethyl cellulose in H_2O (Pavlov et al. 2004), 5 – methyl cellulose in H_2O (Pavlov et al. 1995), 6 – in-here studied CSA samples (Table 1). B – nitrate cellulose (DS \approx 3) in ethyl acetate: 6 – (Hunt et al. 1956), 7 – (Huque et al. 1958), 8 – (Pavlov et al. 1982; Pavlov and Frenkel 1983). The molecular masses M_{sD} by the diffusion-sedimentation analysis were determined in the studies corresponding to (1, 4, 5 and 8) data points, whereas in studies (2, 3, 6, and 7) M_w values were obtained. Empirical envelope lines (polynomials of the second degree) were drawn using these arrays of experimental data

possible types of linear macromolecules (Pavlov et al. 1999; Pavlov 2007). The fundamental Flory-Fox relation: $[\eta] = \Phi_0(\langle h^2 \rangle^{3/2}/M)$ is easily transformed into $[\eta]M_L = \Phi_0(\langle h^2 \rangle^{3/2}/L)$, where L is contour length of the chain. Hence the relation KMHS $[\eta] = K_\eta M^{b_\eta}$ may be turned into $([\eta]M_L) = K_{\eta L} L^{b_\eta}$. This transformation means that the original plot $\lg[\eta]$ vs. $\lg M$ will parallel shift to the left along the $\lg M$ axis on $\lg M_L$ and up on the $\lg[\eta]$ axis also on $\lg M_L$. Obviously, index b_η will not change in this case. Whereas for different polymer systems, the data along $\lg([\eta]M_L)$ axis will be shifted in accordance with, first of all, the length of the statistical Kuhn segment, as well as with thermodynamic quality of the solvent (Pavlov 2007).

The data for different water-soluble cellulose derivatives are shown in Fig. 4. It is clear that all derivatives form virtually single set in more than 300 times range of contour lengths. The totality

of experimental data obtained for methylcellulose (Uda and Meyerhoff 1961; Pavlov et al. 1995), carboxymethyl cellulose (Brown and Henley 1964; Barba et al. 2002), hydroxypropylmethyl cellulose (Pavlov et al. 2004) and CSA (Table 1) form a single dependence of $\lg([\eta]M_L)$ on $\lg L$, which can be described by a second degree polynomial $\lg([\eta]M_L) = (8.0 \pm 0.5) + (1.5 \pm 0.3)\lg L - (0.10 \pm 0.05)(\lg L)^2$, with the correlation coefficient $r = 0.969$.

It means that the volume occupied by unit length of these macromolecules (V/L) is virtually the same for compared derivatives, because the product $[\eta]M_L \sim \langle h^2 \rangle^{3/2}/L \sim V/L$, where V is the volume occupied by macromolecule in solution. In the region of small contour lengths of chains, a trend towards to an increase in the slope of the dependence of $\lg([\eta]M_L)$ vs. $\lg L$ is observed, i.e., an increase in the index b_η ($b_\eta = \Delta \lg([\eta]M_L) / \Delta \lg L = 1.5 - 0.2 \lg L$). Thus, when the contour length changes by two orders of magnitude (from $\lg L_1 = 2.25$ to $\lg L_2 = 4.25$), the index b_η decreases from $b_{\eta 1} \approx 1.0$ to $b_{\eta 2} \approx 0.65$, which is typical for rigid-chain polymer chains and reflects an increase in the degree of permeability of shorter macromolecules. Note that for flexible-chain macromolecules, including flexible-chain polysaccharides in thermodynamically good solvents, the opposite trend will be observed. Namely, upon transition to the region of low molecular masses, the slope of the considered dependence will decrease and tend to 0.5 for flexible-chain macromolecules.

Figure 4 indicates that the chains of compared water soluble cellulose derivatives demonstrate virtually the same equilibrium flexibility. This is explained by the fact that these chains do not contain bulky substituents, and the charged derivatives were studied under conditions of practical suppression of electrostatic interactions.

Besides, Fig. 4 shows data related to studies of highly substituted cellulose nitrates (degree of substitution $\gamma \approx 3$) in ethyl acetate, which are shifted up the Y-axis. This reflects the fact that the molecular chains of highly substituted cellulose nitrates, with the same contour chain length, occupy a larger volume in solution compared to water-soluble cellulose derivatives, i.e. exhibit higher equilibrium stiffness of the chains. As was mentioned above, highly substituted cellulose nitrates are the most rigid polymers among all cellulose derivatives ($A \approx 35 - 40$ nm).

Conclusion

The study of CSA fractions by the methods of molecular hydrodynamics gave a self-consistent spectrum of hydrodynamic characteristics in the 60-fold range of molecular mass. This is an extremely rare homologues set of cellulose derivatives with the mass range in which the change of conformation of the linear chain occurs. The Kuhn-Mark-Houwink-Sakurada relationships were established. Processing of experimental data with Multi-HYDFIT program led to the estimation of the persistent length, hydrodynamic diameter, and shift factor (M_L) characterizing the CSA chains. It is noted that adequate estimates of the M_L value with Multi-HYDFIT program can be obtained only with a sufficient amount of data in the $L/A < 2$ region. An analysis of the literature data for water-soluble cellulose derivatives based on the concept of normalized scaling ratios showed that this group of cellulose derivatives has almost the same equilibrium chain rigidity. The study of CSA short chains has greatly extent the comparable molecular mass range of water-soluble cellulose derivatives. This allowed the appearance of an additional feature in the dependence of the intrinsic viscosity on the chain length, which is characteristic of rigid macromolecular chains.

Author Contributions AG: investigation, data curation, methodology, writing original draft, visualization, review and editing. OO: investigation, data curation, methodology, visualization, review and editing. GK: investigation, methodology. TS: synthesis, methodology. DH: supervision, writing–review and editing. GP: conceptualization, methodology, validation, writing–review and editing, supervision. All co-authors read the manuscript and approved it.

Funding The authors have not disclosed any funding.

Data availability All authors declare that all data and materials support their published claims and comply with field standards.

Declarations

Conflict of interest The authors declare they have no known competing or financial interests or personal relationships that could have appeared to influence the work reported in this paper.

Consent for publication All authors have given approval to the final version of the manuscript.

References

- Amarós D, Ortega A, De La Torre JG (2011) Hydrodynamic properties of wormlike macromolecules: monte carlo simulation and global analysis of experimental data. *Macromolecules* 44:5788–5797. <https://doi.org/10.1021/ma102697q>
- Arca HC, Mosquera-Giraldo LI, Bi V, Xu D, Taylor LS, Edgar KJ (2018) Pharmaceutical applications of cellulose ethers and cellulose ether esters. *Biomacromol* 19:2351–2376. <https://doi.org/10.1021/acs.biomac.8b00517>
- Barba C, Montané D, Farriol X, Desbrières J, Rinaudo M (2002) Synthesis and characterization of carboxymethyl-celluloses from non-wood pulps II. rheological behavior of CMC in aqueous solution. *Cellulose* 9:327–335. <https://doi.org/10.1023/a:1021136626028>
- Brown W, Henley D (1964) Studies on cellulose derivatives. part IV. the configuration of the polyelectrolyte sodium carboxymethyl cellulose in aqueous sodium chloride solutions. *Makromolek Chemie* 79:68–88. <https://doi.org/10.1002/macp.1964.020790107>
- Cantor CR, Schimmel PR (1980) *Biophysical chemistry*. W. H. Freeman and Company, San Francisco
- Cao J, Sun X, Lu C, Zhou Z, Zhang X, Yuan G (2016) Water-soluble cellulose acetate from waste cotton fabrics and the aqueous processing of all-cellulose composites. *Carbohydr Polym* 149:60–67. <https://doi.org/10.1016/j.carbpol.2016.04.086>
- Chauvelon G, Buléon A, Thibault J-F, Saulnier L (2003) Preparation of sulfoacetate derivatives of cellulose by direct esterification. *Carbohydr Res* 338:743–750. [https://doi.org/10.1016/S0008-6215\(03\)00008-9](https://doi.org/10.1016/S0008-6215(03)00008-9)
- Flory PJ (1966) Treatment of the effect of excluded volume and deduction of unperturbed dimensions of polymer chains. configurational parameters for cellulose derivatives. *Makromolek Chemie* 98:128–135. <https://doi.org/10.1002/macp.1966.020980115>
- Geng Y, Almeida PL, Feio GM, Figueirinhas JL, Godinho MH (2013) Water-based cellulose liquid crystal system investigated by rheo-NMR. *Macromolecules* 46:4296–4302. <https://doi.org/10.1021/ma400601b>
- Gilbert RD, Patton PA (1983) Liquid crystal formation in cellulose and cellulose derivatives. *Prog Polym Sci* 9:115–131. [https://doi.org/10.1016/0079-6700\(83\)90001-1](https://doi.org/10.1016/0079-6700(83)90001-1)
- Grinshpan DD, Tret'yakova SM, Tsygankova NG, Makarevich SE, Savitskaya TA (2005) Rheological studies of high-concentration cellulose sulfate-acetate solutions. *J Eng Phys Thermophys* 78:878–884. <https://doi.org/10.1007/s10891-006-0007-3>
- Grinshpan DD, Savitskaya TA, Tsygankova NG, Makarevich SE, Tretsiakova SM, Nevar TN (2010) Cellulose acetate sulfate as a lyotropic liquid crystalline polyelectrolyte: synthesis, properties, and application. *Int J Polym Sci* 2010:831658. <https://doi.org/10.1155/2010/831658>
- Grube M, Cinar G, Schubert US, Nischang I (2020) Incentives of using the hydrodynamic invariant and sedimentation parameter for the study of naturally- and synthetically-based macromolecules in solution. *Polymers* 12:277. <https://doi.org/10.3390/polym12020277>

- Heinze T, Liebert T (2001) Unconventional methods in cellulose functionalization. *Prog Polym Sci* 26:1689–1762. [https://doi.org/10.1016/S0079-6700\(01\)00022-3](https://doi.org/10.1016/S0079-6700(01)00022-3)
- Heinze T, Liebert TF, Pfeiffer KS, Hussain MA (2003) Unconventional cellulose esters: synthesis, characterization and structure-property relations. *Cellulose* 10:283–296. <https://doi.org/10.1023/a:1025117327970>
- Heinze T (2005) In: Dumitriu S (ed) *Polysaccharides: structural diversity and functional versatility* ch. 23. Marcel Dekker, USA, pp 551–590. <https://doi.org/10.1201/9781420030822>
- Hunt ML, Newman S, Scheraga HA, Flory PJ (1956) Dimensions and hydrodynamic properties of cellulose trinitrate molecules in dilute solution. *J Phys Chem* 60:1278–1290. <https://doi.org/10.1021/j150543a031>
- Huque MM, DaI G, Mason SG (1958) Molecular size and configuration of cellulose trinitrate in solution. *Can J Chem* 36:952–969. <https://doi.org/10.1139/v58-137>
- Ishii H, Sugimura K, Nishio Y (2019) Thermotropic liquid crystalline properties of (hydroxypropyl)cellulose derivatives with butyryl and heptafluorobutyryl substituents. *Cellulose* 26:399–412. <https://doi.org/10.1007/s10570-018-2176-6>
- Kádár R, Spirk S, Nypelö T (2021) Cellulose nanocrystal liquid crystal phases: progress and challenges in characterization using rheology coupled to optics, scattering, and spectroscopy. *ACS Nano* 15:7931–7945. <https://doi.org/10.1021/acsnano.0c09829>
- Klemm D, Heublein B, Fink H-P, Bohn A (2005) Cellulose: fascinating biopolymer and sustainable raw material. *Angew Chem Int Ed* 44:3358–3393. <https://doi.org/10.1002/anie.200460587>
- Makarova VV, Tolstykh MY, Picken SJ, Mendes E, Kulichikhin VG (2013) Rheology-structure interrelationships of hydroxypropylcellulose liquid crystal solutions and their nanocomposites under flow. *Macromolecules* 46:1144–1157. <https://doi.org/10.1021/ma301095t>
- Nascimento B, Filho GR, Frigoni ES, Soares HM, Da Silva MC, Cerqueira DA, Valente AJM, De Albuquerque CR, De Assunção RMN, De Castro Motta LA (2012) Application of cellulose sulfoacetate obtained from sugarcane bagasse as an additive in mortars. *J Appl Polym Sci* 124:510–517. <https://doi.org/10.1002/app.34881>
- Ortega A, De La Torre JG (2007) Equivalent radii and ratios of radii from solution properties as indicators of macromolecular conformation, shape, and flexibility. *Biomacromol* 8:2464–2475. <https://doi.org/10.1021/bm700473f>
- Pavlov G, Frenkel S (1995) In: Behlke J (ed) *Analytical ultracentrifugation*. Darmstadt, Steinkopff, pp 101–108. <https://doi.org/10.1007/BFb0114077>
- Pavlov G, Michailova N, Tarabukina E, Korneeva E (1995) Velocity sedimentation of water-soluble methyl cellulose. *Progr Colloid Polym Sci* 99:109–113. <https://doi.org/10.1007/BFb0114078>
- Pavlov G, Zaitseva II, Mikhailova NA (2004) Hydrodynamic and molecular characteristics of hydroxypropylmethyl cellulose and rheology of its aqueous solutions (in Russian). *Polym Sci A* 46:1068–1071
- Pavlov GM, Frenkel SY (1982) About the concentration dependence of macromolecule sedimentation coefficients (in Russian). *Vysokomol Soedin, Ser B* 24:178–180
- Pavlov GM, Kozlov AN, Martchenko GN, Tsvetkov VN (1982) Sedimentation and viscosity of highly substituted cellulose nitrate. *Vysokomol Soed Ser B* 24:284–288
- Pavlov GM, Frenkel SY (1983) Sedimentation velocity of dilute and moderately concentrated solutions of cellulose nitrate. *Polymer Science USSR* 25:1173–1179. [https://doi.org/10.1016/0032-3950\(83\)90017-5](https://doi.org/10.1016/0032-3950(83)90017-5)
- Pavlov GM (1997) The concentration dependence of sedimentation for polysaccharides. *Eur Biophys J* 25:385–397. <https://doi.org/10.1007/s002490050051>
- Pavlov GM, Harding SE, Rowe AJ (1999) In: Cölfen H (ed) *Analytical ultracentrifugation*. Springer, Berlin Heidelberg, pp 76–80. https://doi.org/10.1007/3-540-48703-4_12
- Pavlov GM (2007) Size and average density spectra of macromolecules obtained from hydrodynamic data. *Eur Phys J E* 22:171–180. <https://doi.org/10.1140/epje/e2007-00025-x>
- Pavlov GM, Perevyazko IY, Okatova OV, Schubert US (2011) Conformation parameters of linear macromolecules from velocity sedimentation and other hydrodynamic methods. *Methods* 54:124–135. <https://doi.org/10.1016/j.ymeth.2011.02.005>
- Pavlov GM (2016) In: Uchiyama S, Arisaka F, Stafford W, Laue T (eds) *Analytical ultracentrifugation: instrumentation, software, and applications*. Springer, Japan, pp 269–307. https://doi.org/10.1007/978-4-431-55985-6_14
- Perevyazko I, Gubarev AS, Pavlov GM (2021) Analytical ultracentrifugation and combined molecular hydrodynamic approaches for polymer characterization. *Molecular characterization of polymers*. Elsevier, pp 223–259. <https://doi.org/10.1016/B978-0-12-819768-4.00003-8>
- Rincón-Iglesias M, Lizundia E, Lanceros-Méndez S (2019) Water-soluble cellulose derivatives as suitable matrices for multifunctional materials. *Biomacromol* 20:2786–2795. <https://doi.org/10.1021/acs.biomac.9b00574>
- Rohowsky J, Heise K, Fischer S, Hettrich K (2016) Synthesis and characterization of novel cellulose ether sulfates. *Carbohydr Polym* 142:56–62. <https://doi.org/10.1016/j.carbpol.2015.12.060>
- Savitskaya TA, Nevar TN, Grinshpan DD (2005) Simulation of the rheological behavior of enterosorbents in the gastroenteric tract in vitro. *J Eng Phys Thermophys* 78:989–993. <https://doi.org/10.1007/s10891-006-0023-3>
- Savitskaya TA, Nevar TN, Grinshpan DD (2006) The effect of water-soluble polymers on the stability and rheological properties of suspensions of fibrous activated charcoal. *Colloid J* 68:86–92. <https://doi.org/10.1134/s1061933x0601011x>
- Savitskaya TA, Schakhno EA, Bosko IP, Matulis VE, Melekhovets NA, Grinshpan DD, Ivashkevich OA (2021) Complex formation of kanamycin with cellulose acetate sulfate: a promising path from injectable dosage form to oral. *J Belarus State Univ Chem* 1:3–20
- Seddiqi H, Oliaei E, Honarkar H, Jin J, Geonzon LC, Bacabac RG, Klein-Nulend J (2021) Cellulose and its derivatives:

- towards biomedical applications. *Cellulose* 28:1893–1931. <https://doi.org/10.1007/s10570-020-03674-w>
- Shimamoto S, Uraki Y, Sano Y (2000) Optical properties and photopolymerization of liquid crystalline (acetyl) (ethyl) cellulose/acrylic acid system. *Cellulose* 7:347–358. <https://doi.org/10.1023/a:1009227523297>
- Skazka WS (1985) Sedimentation-diffusion analysis of polymers in solution (in Russian). Publishing house of Leningrad state university, Leningrad
- Sutter W, Kuppel A (1971) Zum einfluß der molekularen uneinheitlichkeit auf molekulargewichtsabhängige eigenschaften von polymeren in lösung. *Makromolek Chemie* 149:271–289. <https://doi.org/10.1002/macp.1971.021490122>
- Tanford C (1961) Physical chemistry of macromolecules. Wiley, New York
- Thomas M, Chauvelon G, Lahaye M, Saulnier L (2003) Location of sulfate groups on sulfoacetate derivatives of cellulose. *Carbohydr Res* 338:761–770. [https://doi.org/10.1016/S0008-6215\(03\)00010-7](https://doi.org/10.1016/S0008-6215(03)00010-7)
- Tsvetkov VN (1969) Semi-rigid chain molecules. *rus. Chem Rev* 38:755–773. <https://doi.org/10.1070/RC1969v038n09ABEH001835>
- Tsvetkov VN, Eskin VE, Frenkel SY (1971) Structure of macromolecules in solution. *Nat. Lend. Library Sci. & Technol.*, Boston
- Tsvetkov VN, Lavrenko PN, Bushin SV (1984) Hydrodynamic invariant of polymer molecules. *J Polym Sci Part A Polym Chem* 22:3447–3486. <https://doi.org/10.1002/pol.1984.170221160>
- Tsvetkov VN (1989) Rigid-chain polymers: hydrodynamic and optical properties in solution. Consultants Bureau, New York. <https://archive.org/details/rigidchainpolyme0000tsve/page/n7/mode/2up>
- Uda VK, Meyerhoff G (1961) Hydrodynamische eigenschaften von methylcellulosen in lösung. *Makromolek Chemie* 47:168–184. <https://doi.org/10.1002/macp.1961.020470115>
- Werbowj RS, Gray DG (1976) Liquid crystalline structure in aqueous hydroxypropyl cellulose solutions. *Mol Cryst Liq Cryst* 34:97–103. <https://doi.org/10.1080/15421407608083894>

Publisher's Note Springer Nature remains neutral with regard to jurisdictional claims in published maps and institutional affiliations.

Springer Nature or its licensor (e.g. a society or other partner) holds exclusive rights to this article under a publishing agreement with the author(s) or other rightsholder(s); author self-archiving of the accepted manuscript version of this article is solely governed by the terms of such publishing agreement and applicable law.